J Mater Cycles Waste Manag
DOI 10.1007/s10163-017-0661-x

ORIGINAL ARTICLE

Experimental study on reuse of recycled concrete aggregates for load-bearing components of building structures

Feng Liu[1] · Yin-Yin Yu[2] · Li-Juan Li[1] · Lan Zeng[1]

Received: 11 March 2017 / Accepted: 20 August 2017

Abstract Recycled aggregates recovered from abandoned buildings or demolished concrete structures were reused to produce concrete columns as new building components. A quasi-static test on 10 recycled aggregate concrete filled steel tubular (RACFST) columns was carried out. The mechanical properties of RACFST columns in the study include failure mode, hysteretic loops, skeleton curves, stiffness deterioration curves and energy dissipation capacity. RACFST columns with different recycled aggregate replacement ratios were tested under constant axial load and cyclic lateral load. The seismic performance of the columns was analyzed. The experimental results indicate that concrete adding recycled aggregates does not reduce the lateral stiffness of the columns, and their energy dissipation capacity is nearly as good as that of natural aggregate concrete filled steel tubular columns. The usage of recycled aggregate concrete has little influence on the lateral load-bearing capacity and the stiffness deterioration of RACFST columns. The current calculation for natural aggregate concrete filled steel tubular columns to estimate the lateral load-bearing capacity of RACFST columns tends to be relatively conservative. The reuse of recycled aggregates for load-bearing components of building structures especially for concrete filled steel tubular columns is feasible.

Keywords Demolished concrete structures · Recycled aggregates · Concrete filled steel tubular columns · Mechanical property

Introduction

The rapid development of urbanization in China results in a large amount of demolished building materials, in which concrete is the most. However, the recycled aggregates recovered from abandoned buildings or demolished concrete structures can be reused to produce recycled concrete if properly treated such as crushing, washing, sieving and grading. The aggregate made from abandoned buildings or demolished concrete structures can be used to replace some or all of the coarse aggregate in concrete mixture to form recycled aggregate concrete (RAC). Up to now, extensive researches have been carried out on the mechanical properties of RAC, including the study of recycled concrete members and structures. It was shown that RAC could be used mainly in the structures with lower stress or force level because of the characteristic limitations of recycled aggregate itself [1, 2]. However, thanks to the combination of RAC and concrete filled steel tubular (CFST) structures, which has been put forward by researchers and instantly aroused an interest in practice [3], the method of filling the steel tube with recycled aggregate concrete or demolished concrete lumps partially or wholly not only reduces the whole weight of buildings, but also decreases the price of concrete members [4]. As the recycled aggregate has a

✉ Li-Juan Li
lilj@gdut.edu.cn

Feng Liu
fliu@gdut.edu.cn

Yin-Yin Yu
50438341@qq.com

Lan Zeng
1050550263@qq.com

[1] School of Civil and Transportation Engineering, Guangdong University of Technology, Guangzhou 510006, China

[2] Architectural and Structure Design Research Center, Architectural Design and Research Institute of Guangdong Province, Guangzhou 510006, China

Published online: 07 September 2017

positive influence on the ductility of RAC structures [5], it is desired to apply on the buildings with high seismic resistance requirements or the areas with frequent destructive earthquakes. Meanwhile, recycled aggregate concrete is considered to provide high and obvious economic and social benefits and promising application prospect [6].

The basic mechanism of RAC filled steel tubular (RACFST) members is similar to the situation of natural aggregate concrete filled steel tubular members, and tests for the material have shown that the Poisson's ratio of RAC is nearly the same as that of natural aggregate concrete [7], which tends to indicate that the steel tube can be applied on confining RAC as it does for natural aggregate concrete. A series of investigations on the mechanical property, durability and structural performance of RACFST columns have been carried out in the past 15 years after initially studied in the late 90's [8]. The related studies are ranged on the mechanical performance of RACFST columns, especially under axial or eccentric compression [9–12], the shrinkage and creep of the core concrete [13], the working mechanism of steel tube confinement [14, 15], the energy dissipation capacity of RACFST columns [16, 17], and so on. The seismic resistant performance of RACFST columns is also one of the critical issues to work out before the wide application of these composites, and the mechanism of RAC, including the adhering mechanism and fracture property between recycled aggregate and cementitious materials, as well as its durability, has great effect on the dynamic mechanical property of RACFST columns, which is the main concern among engineers when RAC is used into structures [18, 19]. However, since the performances of RAC has large discreteness and are greatly affected by structural aging properties, the study of mechanical and dynamical properties of RACFST columns is limited up to now.

In this paper, a quasi-static test was conducted for 10 RACFST columns with 165 mm in diameter, steel tubes with 4 mm and 2 mm in thickness, respectively. The specimens were designed on the slenderness ratio and axial compression ratio of columns which was commonly used in projects. Different recycled coarse aggregate (RCA) replacement ratios and steel ratios were chosen as testing parameters. The failure mode, hysteresis property, skeleton curves, ductility coefficient, stiffness deterioration curves and energy dissipation capacity of RACFST under both constant axial compression and cyclic lateral loading were obtained. The seismic performance of RACFST was analyzed.

Experimental program

Material properties

The following materials were used in the test: ordinary Portland cement with 42.5 MPa compressive strength, river sand with a maximum size of 5 mm and a fineness

Table 3 Main properties of steel tubes

Thickness (mm)	Ultimate strength (MPa)	Yield strength (MPa)	Elastic modulus (MPa)	Elongation (%)
4	440	340	228 × 103	13.12
2	580	490	240 × 103	13.78

Table 1 Margin specifications

Type	Size (mm)	Apparent density (kg/m^3)	Bulk density (kg/m^3)	Water absorption (%)	Crushing index (%)
Original coarse aggregate	≤10	2785	1448	0.75	4.54
Recycled coarse aggregate	≤10	2456	1287	4.12	15.72

Table 2 Mix proportion of concrete

Concrete	Contents Per cubic							Water–cement ratio	Sand percentage (%)
	Cement	Water	Sand	Fly ash	Recycled aggregate	Coarse aggregate	Water reducing agent		
M0	330	156	710	120	–	1064	9	0.35	0.4
M30	330	156	710	120	319	745	9	0.35	0.4
M50	330	156	710	120	532	532	9	0.35	0.4

In Mr, M refers to the RAC, and r refers to the concrete with a RCA replacement ratio of r(%). For example, M30 means the concrete with the RCA replacement ratio of 30%

Table 4 Design of specimens

Specimen	$D \times t \times L$ (mm)	D/t	Slenderness	RCA replacement ratio (%)	Steel ratio
HM0-1	165 × 4 × 1200	41.25	29.09	0	0.105
HM0-2	165 × 4 × 1200	41.25	29.09	0	0.105
HM30-1	165 × 4 × 1200	41.25	29.09	30	0.105
HM30-2	165 × 4 × 1200	41.25	29.09	30	0.105
HM50-1	165 × 4 × 1200	41.25	29.09	50	0.105
HM50-2	165 × 4 × 1200	41.25	29.09	50	0.105
BM30-1	165 × 2 × 1200	82.50	29.09	30	0.05
BM30-2	165 × 2 × 1200	82.50	29.09	30	0.05
BM50-1	165 × 2 × 1200	82.50	29.09	50	0.05
BM50-2	165 × 2 × 1200	82.50	29.09	50	0.05

In HMr-n and BMr-n, H refers to the thick-walled steel tube, B refers to the thin-walled steel tube, and n refers to the specimen number in the same group

Table 5 Strength of concrete

Test cube of specimen	f_{cu1} (MPa)	f_{cu2} (MPa)	f_{cu3} (MPa)	f_{cu} (MPa)
M0-1	55.4	54.9	55.0	55.1
M0-2	57.9	56.7	55.9	56.8
M30-1	55.7	63.1	58.9	59.3
M30-2	56.4	58.6	63.3	59.4
M50-1	56.1	64.8	51.1	57.3
M50-2	58.7	54.8	62.8	58.8

M0-2, M30-2 and M50-2 refer to the concrete cube strength of M0, M30 and M50 for 180 days corresponding. M0-1, M30-1 and M50-1 refer to the concrete cube strength of M0 (55 days), M30 (67 days) and M50 (72 days) when the, respectively, specimens was being loaded

modulus of 2.6, the crushed stone aggregate and RCA with continuous grading and a maximum size of 10 mm. The RCA was provided by a manufacture as industrial products from a building worked over 20 years. The main properties of coarse aggregate are shown in Table 1. The mixture proportion of concrete is shown in Table 2. The material properties of steel tube are shown in Table 3.

Specimen design

Ten RACFST specimens with a rigidly supported base were designed. The design details of each specimen are shown in Table 4. The test cubes with a side length of 150 mm were cast simultaneously and their strength was shown in Table 5. The strength of the concrete with the RCA replacement ratio of 30% (M30) is a little higher than that of the M50 and

Table 6 Basic parameters of specimens

Specimen	f_a (MPa)	f_c (MPa)	θ	N (kN)	N_u (kN)	n
HM0-1	308.0	36.9	0.9	320.0	1585.9	0.20
HM0-2	308.0	36.9	0.9	300.0	1585.9	0.19
HM30-1	308.0	39.6	0.8	320.0	1647.9	0.19
HM30-2	308.0	39.6	0.8	290.0	1647.9	0.18
HM50-1	308.0	38.3	0.8	290.0	1619.0	0.18
HM50-2	308.0	38.3	0.8	320.0	1619.0	0.20
BM30-1	343.0	39.6	0.4	230.0	1338.1	0.17
BM30-2	343.0	39.6	0.4	260.0	1338.1	0.19
BM50-1	343.0	38.3	0.5	240.0	1310.3	0.18
BM50-2	343.0	38.3	0.5	230.0	1310.3	0.18

$f_c = 0.88 \times 0.76 \times f_{cu}$; $\theta = f_a A_a / f_c A_c$,where A_c is the cross sectional area of core concrete and A_a is the cross sectional area of steel tube.$N_u = \phi_1 \phi_2 N_0$, where, N_0 is the design value of axial compression of the CFTC column, which can be calculated as $N_0 = f_c A_c (1 + \sqrt{\theta} + \theta)$; ϕ_2 is the reduction factor of load-bearing capacity effected by slenderness ratio, which can be given as $\phi_2 = 1 - 0.115\sqrt{l_c/d - 4}$; ϕ_1 is the reduction factor of load-bearing capacity effected by eccentricity. $n = N/N_u$

Fig. 1 Test set-up and instruments

the natural aggregate concrete M0 for the same age. The concrete strength of all three batches is increased with time passes, but the increase of the M30 strength is less than the other two.

Basic parameters

The basic parameters of specimens are shown in Table 6, where f_a is the design value of tensile and compressive strength of steel tubes, f_c is the design value of compressive strength of concrete, θ is the confinement coefficient of concrete filled steel tubes, N is the average value of axial force loaded, N_u is the design value of load-bearing capacity of the CFST column, and n is the axial load ratio (the ratio of axial load to ultimate axial load) which can be calculated from

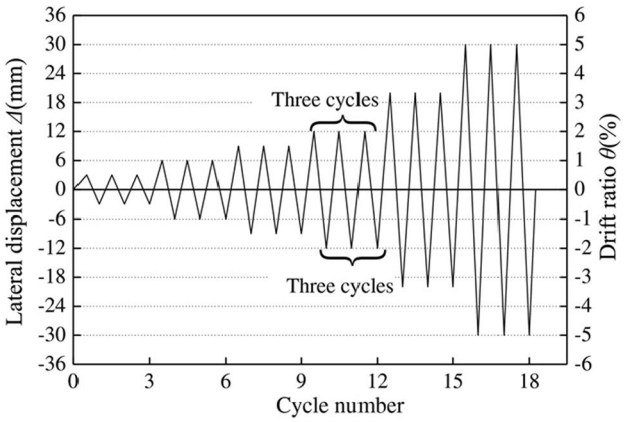

Fig. 3 Displacement history for testing

DG/TJ 08-2018-2007 [20] and DB34/T1262-2010 [21]. The designed axial load ratio is 0.2, while the actual value has some fluctuations in the test process.

Set-ups and loading system

The axial compression was loaded through a hydraulic jack with the capacity of 5000 kN, while the lateral force was exerted by the American MTS system which is shown in Fig. 1.

Three groups of linear voltage displacement transducers (LVDTs) were set in the lateral loading point on top of the column, the middle and the bottom position of the column in both vertical and horizontal directions, respectively, to measure the displacements in testing. 26 strain gauges were pasted on the surface of each steel tube to obtain the tensile, compression and torsion strains of the column. The schematic diagram of strain gauges location is shown in Fig. 2. The strains and displacements were obtained automatically by TDS system. According to JGJ101-96 [22], the loading method by load control was used at the beginning, then the

Fig. 2 Schematic diagram of strain gauges location

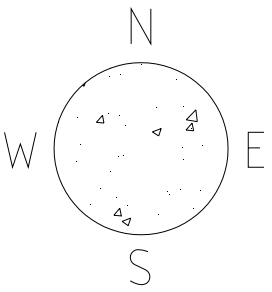

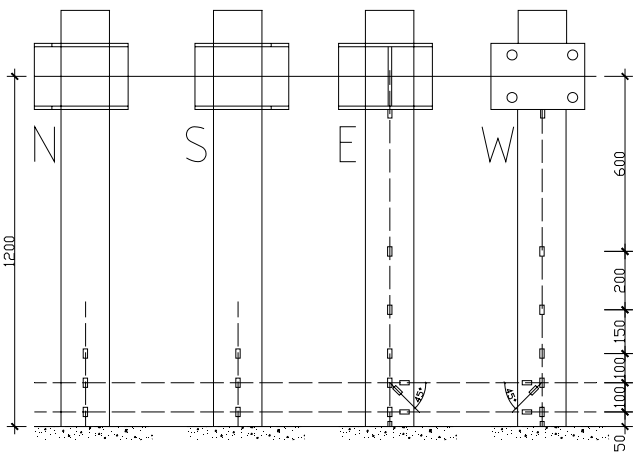

Fig. 4 Failure mode of specimen

loading method by displacement control was adopted later. The displacement history for testing is shown in Fig. 3.

Experimental results and analysis

Failure mode of specimens

The failure process of RACFST columns was similar to that of CFST columns, and the failure mode is shown in Fig. 4. Local buckling like the shape of "elephant's leg" took place at the place of 20 mm above the column bottom. The local buckling of the RAC filled thin-walled steel tubular columns (the BM column series) appeared earlier than that of the RAC filled thick-walled steel tubular columns

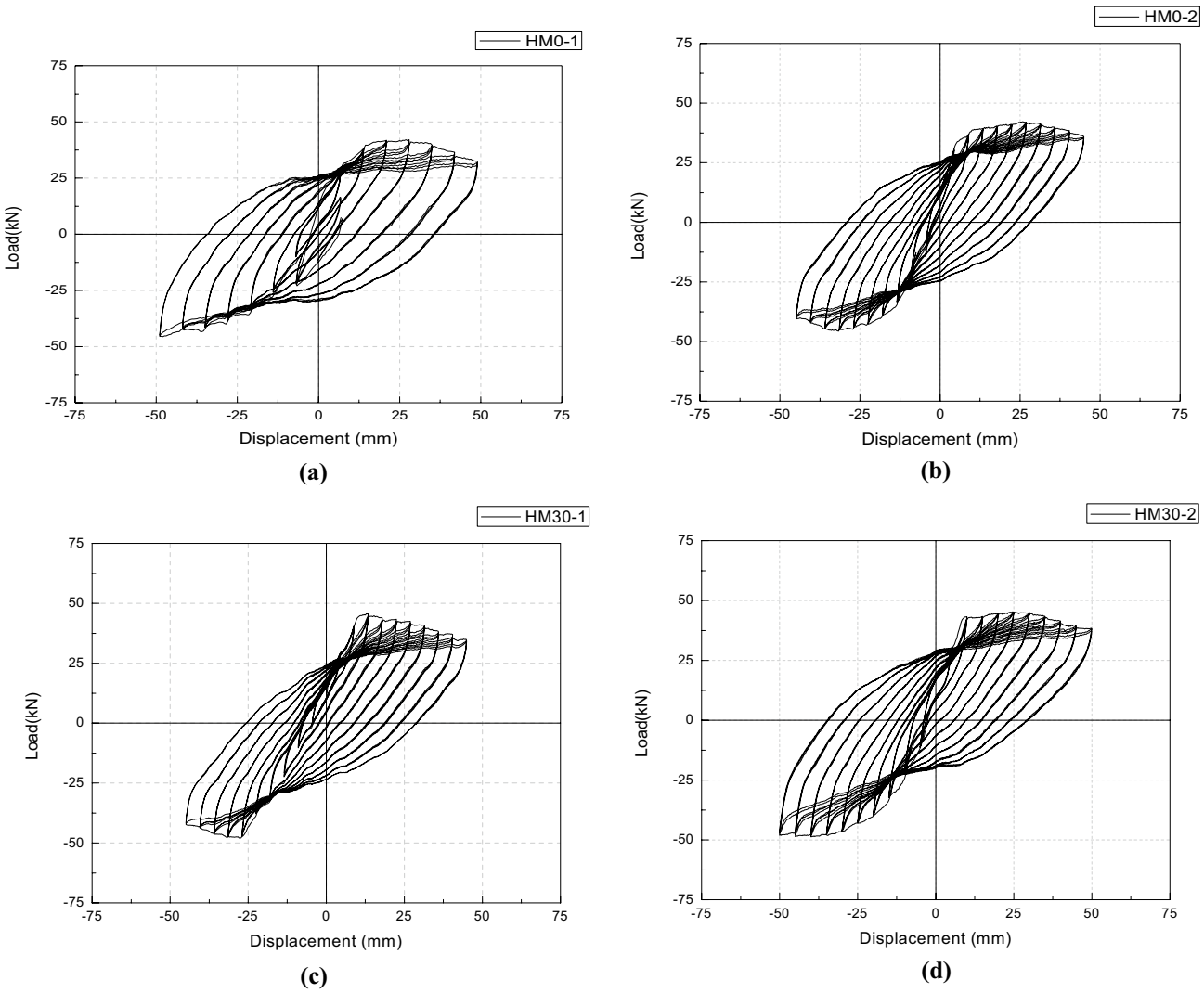

Fig. 5 Hysteretic loops of RACFST columns: **a** hysteretic loops of HM0-1; **b** hysteretic loops of HM0-2; **c** hysteretic loops of HM30-1; **d** hysteretic loops of HM30-2; **e** hysteretic loops of HM50-1; **f** hysteretic loops of HM50-2; **g** hysteretic loops of BM30-1; **h** hysteretic loops of BM30-2; **i** hysteretic loops of BM50-1; **j** hysteretic loops of BM50-2

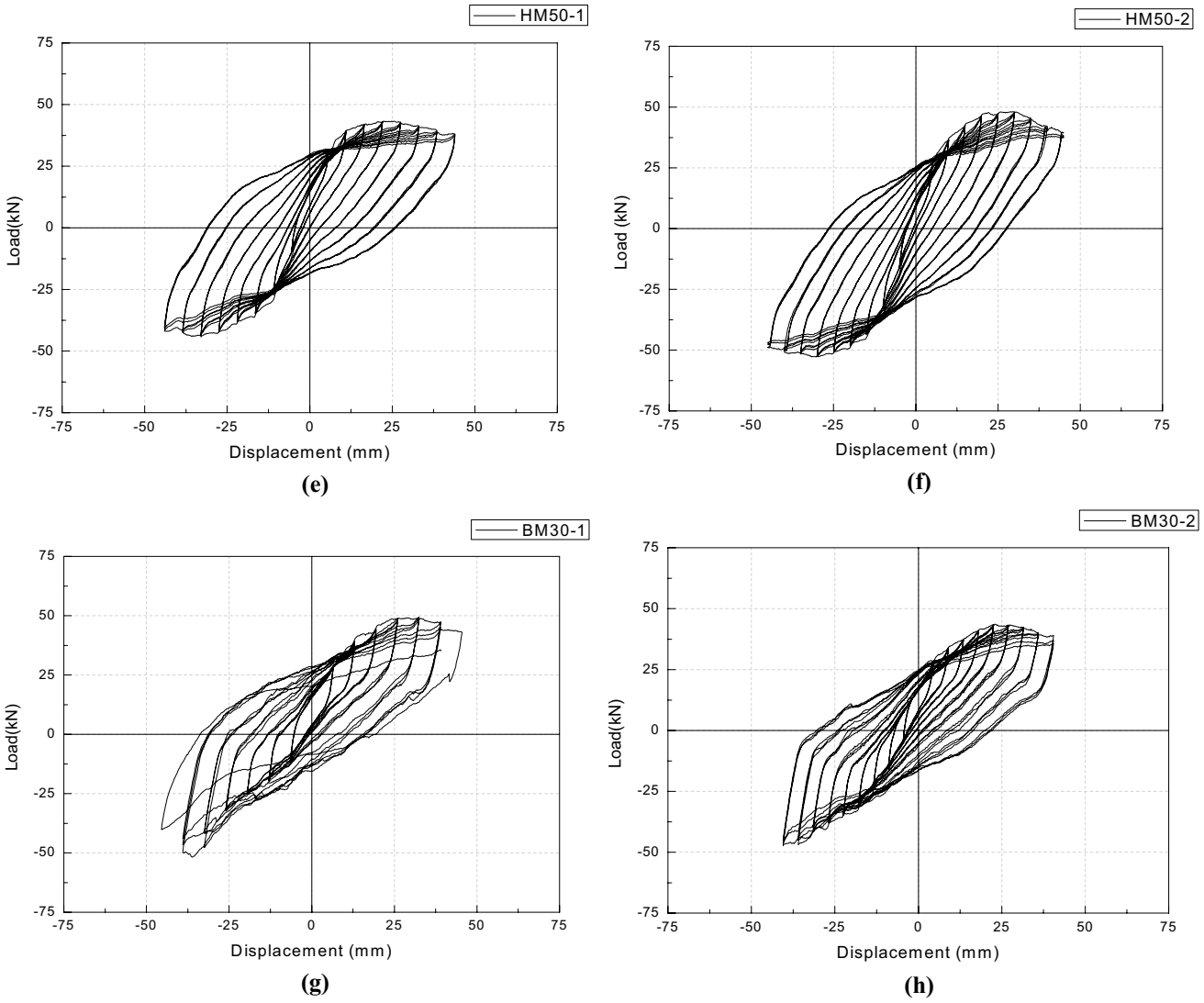

Fig. 5 (continued)

(the HM column series). Little local buckling showed up on the surface of the compression zone at the bottom of the BM columns when the lateral displacement becomes 2 times the lateral yield displacement ($2\Delta_y$). The bulking extended gradually to the wall of the steel tube on the side of the compression zone with an increase of displacement. The shape of local buckling in BM columns was narrow and slim compared with that of thicker wall ones. The bulking area of the BM columns expanded rapidly when the lateral displacement reaches to $5\Delta_y$, and finally the lateral confinement of steel tubes had no effect any longer. There was no obvious difference between the HM columns and the CFST columns when local buckling happens. The appearance of local buckling for the BM columns with different RCA replacement ratios was nearly at the same time, which indicated that the RCA replacement ratio had little effects on the local buckling of steel tubes. Compared with the BM column series, the local buckling of the HM column series appeared later, which reflected the core concrete in the HM column series took effect later. Since the core concrete in HM columns series took less responsibility on bearing loads, the RCA replacement ratios of the HM column series had little influence on their failure behavior. Thus, local buckling is a critical issue to govern the ultimate state behavior of specimens.

Hysteretic loop

The load–displacement hysteretic loops of RACFST columns are shown in Fig. 5. It can be seen from Fig. 5 that the hysteretic performance of the RACFST columns is nearly as good as that of the CFST ones. The pinch phenomenon

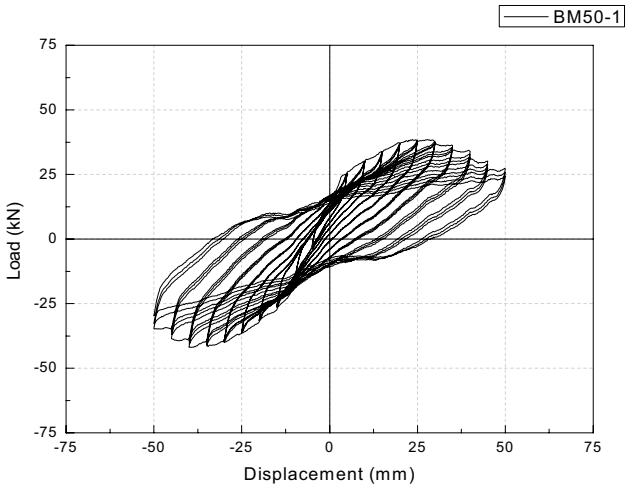

(i)

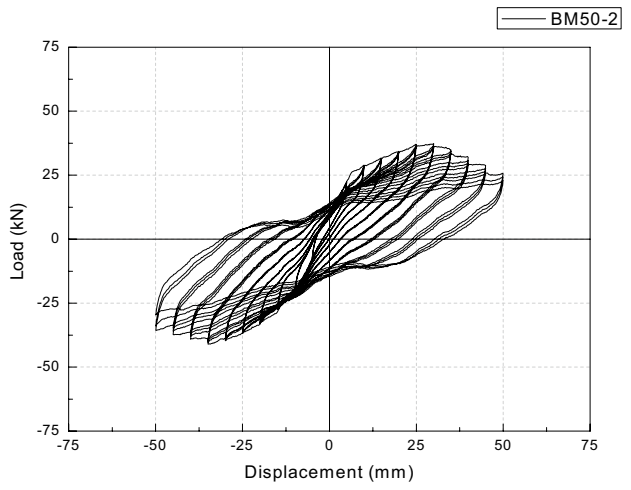

(j)

Fig. 5 (continued)

happens when the BM columns have large deformation. However, the load-bearing capacity of the BM columns, which was designed according to CECS28:90 [23], does not drop down sharply before their failure. Thanks to the reliable confinement of steel tubes and interaction between the steel tube and the core concrete, the seismic performance of RACFST columns is fully shown out. Moreover, the elastic stiffness and seismic load-bearing capacity of RACFST columns increased with the increase of steel ratio. In contrast to the BM columns, the speed of load-bearing capacity degradation for the HM columns is slower, and there is no obvious pinch phenomenon, which can be told from the round hysteresis loop. The deterioration of strength and stiffness of the HM columns is not obvious even with large deformation. In the HM column series, the lateral load-bearing capacity of columns is inversely proportional to the strength of the core concrete; however, the situation is completely different for the series of BM columns, which may be caused by the more load-bearing core concrete compared with the HM columns.

In this test, it can be seen from Table 6 that the compressive strength of concrete with RCA replacement ratios of 30 and 50% is higher than that of natural aggregate concrete. This may result from higher water absorption of RCA which makes the actual water–cement ratio of RAC lower than it being designed. It also reflects the instability of the properties of RCA from which the RAC were derived [24]. The recycled aggregate affects the hysteretic performance and ductility of the columns but has no direct relations with the RCA replacement ratio. The hysteretic performance becomes worse with the increase of concrete strength for the HM columns, however, for the BM columns, the hysteretic loops of the BM30 columns show better performance than that of the BM50 ones. Besides, the declining tendency of the load-bearing capacity of the BM50 columns is smooth after damage, which suggests that the interaction between steel tubes with core concrete is more reliable for the RCA replacement ratio of 50% than that for 30%.

Skeleton curves and ductility

The ductility coefficient of each column is shown in Table 7. The lateral load–displacement skeleton curves are shown in Fig. 6.

For the HM columns, the RCA replacement ratio has little effect on the initial part of the skeleton curve, which means that recycled aggregate has little effect on the lateral stiffness of RACFST columns. The lateral load-bearing capacity of the HM columns is higher than that of the CFST columns. However, the skeleton curves of the HM columns drop faster than that of the CFST columns after the peak point, thus the ductility coefficient of the latter is a little bit larger than the former. The situation is changed for the BM columns that the RCA replacement ratio has a certain effect on the initial part of the skeleton curve but has little influence on the lateral stiffness of columns.

For the columns with the RCA replacement ratio of 30%, the ductility of HM30 is better than that of BM30, while the load-bearing capacity is almost the same. In this test, the tensile strength of thin-wall steel tubes is higher than that of the thick-wall ones, so both the lateral load-bearing capacities and skeleton curves of two type of steel tubes are similar in the decreasing phase. Obviously, the thick-wall steel tubes carried more axial compression than the thin-wall ones, so for the same axial load ratio, more axial loads of thick-wall steel tubes are transferred to the core concrete when local buckling happens. If all the axial compression is taken by the core concrete, ignoring the axial load-bearing capacity of steel tubes after local buckling, the axial load ratio of the core concrete increases sharply, from 0.19 to 0.42 for HM30-1 and from 0.19 to

Table 7 The ductile coefficients

Specimen	P_{ue1}	P_{ue2}	P_{ue}	Δ_u	Δ_y	u	P	P/P_{ue1}
HM0-1	–	–	–	–	–	–	–	–
HM0-2	42.22	−45.76	43.99	43.81	4.43	9.89	38.19	1.11
HM30-1	44.77	−48.07	46.42	33.93	4.45	7.62	40.38	1.11
HM30-2	45.34	−48.67	47.00	45.52	5.01	9.09	40.07	1.13
HM50-1	43.29	−44.23	43.76	45.54	5.48	8.31	40.53	1.07
HM50-2	48.13	−52.80	50.47	41.62	5.03	8.27	37.50	1.28
BM30-1	49.38	−51.83	50.61	37.49	6.50	5.77	28.68	1.72
BM30-2	43.71	−46.37	45.04	45.13	5.29	8.53	24.69	1.77
BM50-1	38.49	−41.93	40.21	38.08	5.01	7.62	26.98	1.43
BM50-2	37.29	−41.00	39.15	37.98	5.00	7.60	27.03	1.38

The data of specimen HM0-1 are unreliable because of the loading machine, which are omitted. P_{ue1} and P_{ue2} are load-bearing capacity on the loading direction and its opposite side, respectively. P_{ue} is the absolute average value of P_{ue1} and P_{ue2}. Δ_u is the damage displacement corresponding to the minimum of the three absolute values of $0.85P_{ue1}$, $0.85P_{ue2}$ and $0.85P_{ue}$. P is the lateral load-bearing capacity of specimens calculated by DB34/T1262-2010 [21]. $P = M_u/L$,where M_u refers the ultimate moment of the CFST columns, which can be calculated as $M_u = \gamma_m W f_a$, where γ_m is the flexural plastic development coefficient, calculated as $\gamma_m = 1.1 + 0.48\ln(\xi + 0.1)$, and W is the elastic section modulus. u is ductility coefficient $u = \Delta_u/\Delta_y$

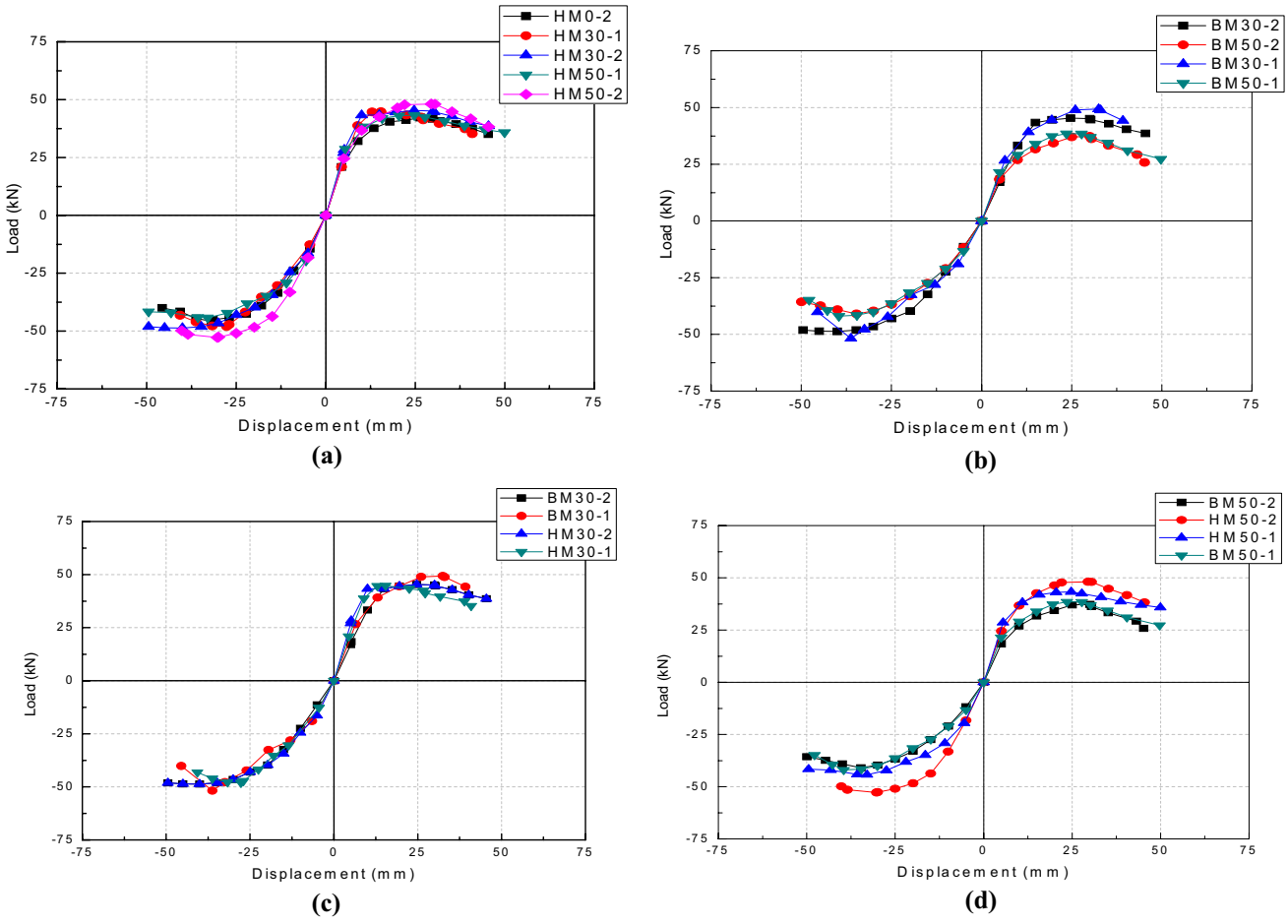

Fig. 6 Skeleton curves: **a** skeleton curves of HM columns; **b** skeleton curves of BM columns; **c** skeleton curves of RCA replacement ratio of 30%; **d** skeleton curves of RCA replacement ratio of 50%

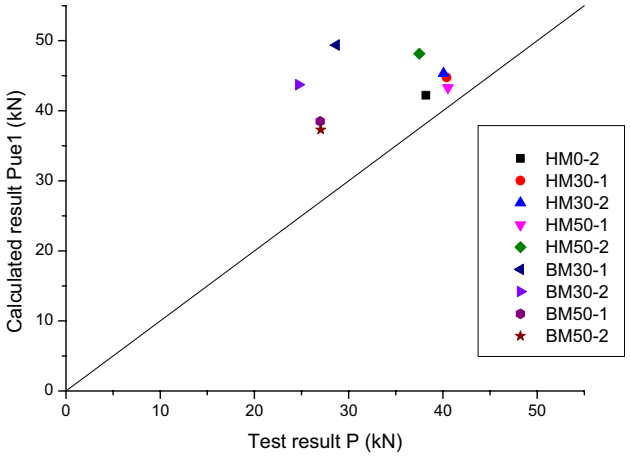

Fig. 7 Comparison of calculated and test results of lateral load-bearing capacity

0.32 for BM30-2. The local bulking makes the confinement effect weaker, which cannot take advantage of thick-wall steel tubes. For the columns with the RCA replacement ratio of 50%, both ductility and lateral load-bearing capacity of the HM columns is generally better than that of the BM ones. However, for reverse loading cases, the skeleton curves of specimens HM50-1 and BM50-1 are almost coincided, with a similar reason explained above.

The lateral load-bearing capacity of the HM columns matched well with the data calculated from DB34/T1262-2010 [21], which is used for the CFST columns. From Fig. 7 and the ratios of the calculated values P to the test results P_{ue1} in Table 7, the test results are generally a little bit larger than the calculated ones, with the ratios of test data to calculation values being 1.07–1.28, which indicates it is rational to use the current standard to calculate the lateral load-bearing capacity of RAC filled thick-wall steel tubular columns. For the lateral load-bearing capacity of BM columns, the ratios of test data to calculation values are 1.72–1.77 and 1.38–1.43 for the BM30 and

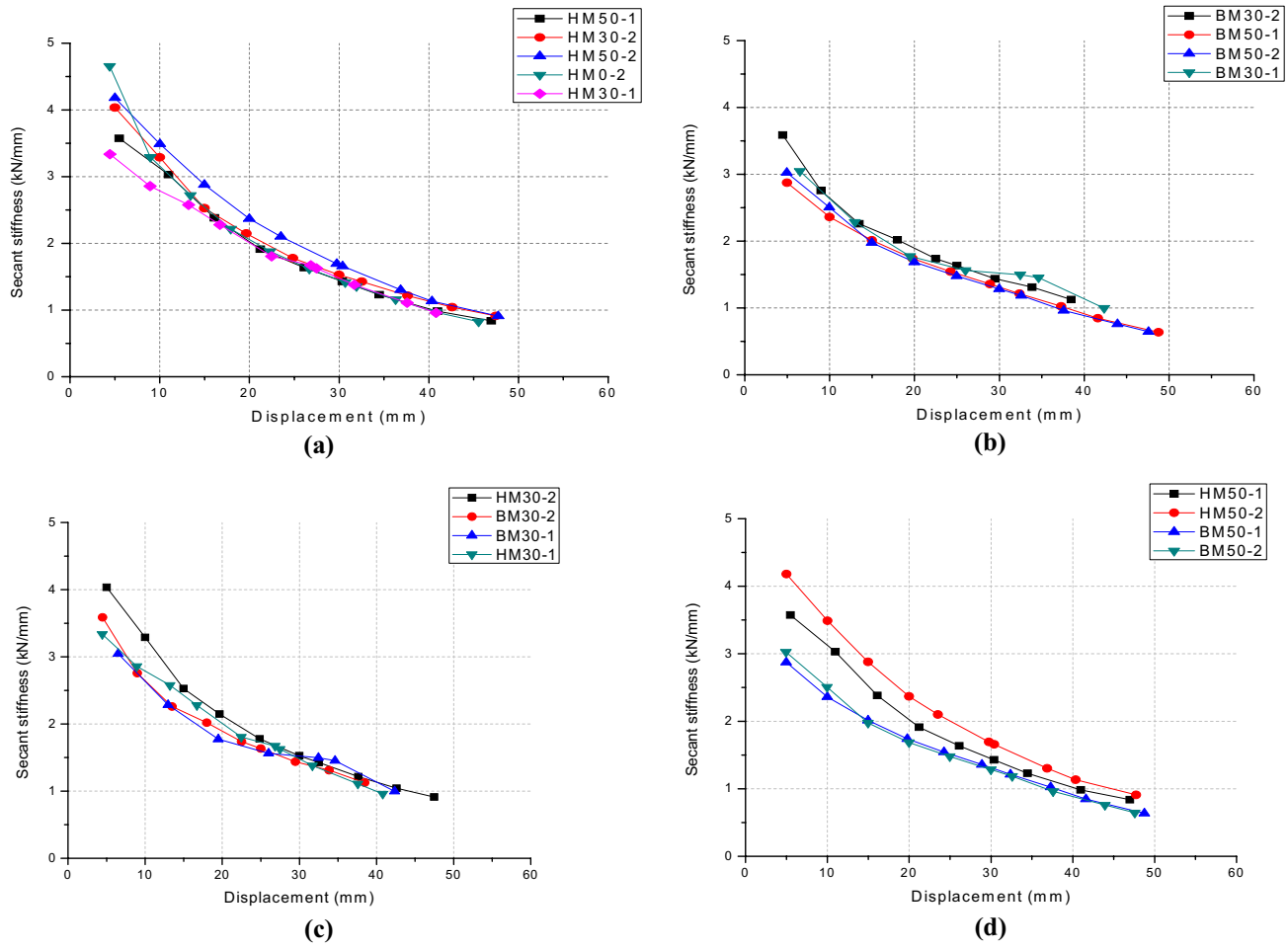

Fig. 8 Stiffness deterioration: **a** stiffness deterioration of HM; **b** stiffness deterioration of BM; **c** stiffness deterioration of M30; **d** stiffness deterioration of M50

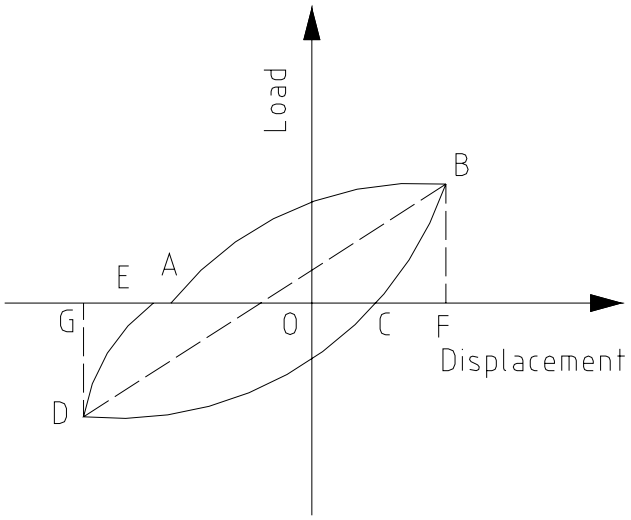

Fig. 9 Diagram of the energy dissipation

BM50 columns, respectively. It shows that the lateral load-bearing capacity of recycled concrete filled thin-wall steel tubular columns from the calculation tends to be relatively conservative.

Curves of stiffness deterioration

Curves of stiffness deterioration of columns are shown in Fig. 8. It can be seen from Fig. 8 that the stiffness degradation occurs mainly in the cyclic loading of level $1\Delta_y$, $2\Delta_y$ and $3\Delta_y$, and then it slows down with the increase of lateral displacement. The RCA replacement ratio has little effect on the stiffness degradation curves for columns with different thickness of tubes. Stiffness deterioration curves are substantially the same for columns with the same steel ratio. The first cycle peak stiffness of the HM columns are lower than that of the CFST columns at the first-level displacement, and the first cycle peak stiffness of the HM30 columns is lower than that of the HM50 ones, which is similar to the BM columns. The influence of steel ratio on stiffness deterioration curves for columns with the same RCA replacement ratios is similar. The peak stiffness of the HM columns is higher than that of the BM ones. The deterioration of stiffness occurred mainly in the earlier cycles, especially for the M50 columns.

Capacity of energy dissipation

In this paper, energy dissipation coefficient and equivalent viscous damping are calculated by the first hysteresis loop of the displacement amplitude corresponding to the peak load and the failure load, respectively, as shown in Fig. 9. The energy dissipation coefficient E and equivalent viscous damping ξ_{eq} were calculated according to Eqs. (1) and (2) [21]. The detailed calculation results are shown in Table 8.

$$E = S_{ABCDEA} \big/ (S_{\Delta OBF} + S_{\Delta ODG}) \tag{1}$$

$$\xi_{eq} = \frac{E}{2\pi} = \frac{1}{2\pi} \frac{S_{ABCDEA}}{(S_{\Delta OBF} + S_{\Delta ODG})} \tag{2}$$

It can be seen from Table 8 that the values of equivalent viscous damping range from 0.255 to 0.320 and 0.203 to 0.263 for the HM columns and the BM ones, respectively, and the equivalent viscous damping of reinforced concrete columns is usually 0.1–0.2, which shows that the energy absorption capacity of RACFST columns is as good as the normal concrete columns. The energy dissipation capacity of the HM columns is inversely proportional to the strength of the core concrete under the same steel ratio, while for the BM columns, the trend is on the contrary. In general, the capacity of energy dissipation of the two M30 columns is variable, but the M0 and M50 columns reveal similar energy consumption capacity.

Table 8 Coefficient of energy dissipation and equivalent viscous damping

Specimen	Peak hysteresis loop				Failure hysteresis loop				E_t
	S_{ABCDEA}	$S_{\Delta OBF} + S_{\Delta ODG}$	E	ξ_{eq}	S_{ABCDEA}	$S_{\Delta OBF} + S_{\Delta ODG}$	E	ξ_{eq}	
H0-2	1352.20	1157.39	1.168	0.186	3776.90	1851.16	2.040	0.325	45669
H30-1	301.09	447.06	0.673	0.107	2624.10	1635.61	1.604	0.255	30995
H30-2	1072.19	1099.69	0.975	0.155	3654.64	2162.84	1.690	0.269	41704
H50-1	1395.02	1171.36	1.191	0.190	4361.11	2182.41	1.998	0.318	43252
H50-2	1835.10	1509.68	1.216	0.194	4280.65	2130.00	2.010	0.320	43994
B30-1	1924.45	1475.50	1.304	0.208	521.80	394.00	1.324	0.211	24029
B30-2	1109.30	1098.54	1.010	0.161	2621.82	1588.60	1.650	0.263	28922
B50-1	871.07	1166.85	0.747	0.119	1967.80	1544.46	1.274	0.203	20983
B50-2	944.16	1153.36	0.819	0.130	2017.50	1484.71	1.359	0.216	21297

E is the energy dissipation coefficient, E_t is the total energy consumption and ξ_{eq} is the equivalent viscous damping

Conclusion

From the analyses of hysteresis loops, skeleton curves, ductility, stiffness deterioration and energy dissipation based on the experimental results of 10 RACFST columns under constant axial compression and cyclic lateral loading, the following conclusions can be obtained.

1. RCA replacement ratio has little effect on the lateral load-bearing capacity of RACFST columns, but the compressive strength of the core concrete does. Adding RCA does not reduce the lateral stiffness of RACFST columns, and the curves of stiffness deterioration with different RCA replacement ratios are substantially the same at the same steel ratio.
2. The energy dissipation capacity of RACFST columns, including those with the thin-wall steel tubes, is not inferior to that of the CFST columns. The steel ratio has a more significant influence on the energy dissipation for the RACFST columns with a RCA replacement ratio of 30% than that with a ratio of 50%, while it has a similar influence on the stiffness deterioration and has little effect on the lateral load-bearing capacity of RACFST columns with different RCA replacement ratios.
3. It is rational to use the current standard DB34/T1262-2010 for the CFST columns to calculate the lateral load-bearing capacity of RAC filled thick-wall steel tubular columns, but it tends to be relatively conservative for the recycled concrete filled thin-wall steel tubular columns.
4. It is technically feasible for recycled aggregate coming from waste building materials to produce concrete filled steel tubular columns, which presents a possible method for high valuable reuse of waste materials in building structures for load-bearing components.

Acknowledgements This research was jointly funded by the National Natural Science Foundation of China (Project nos. 51278132, 11472084) and Science and Technology Planning Project of Guangzhou City (Project no. 201704030057). These foundations are greatly appreciated.

References

1. Silva RV, De Brito J, Dhir RK (2014) Properties and composition of recycled aggregates from construction and demolition waste suitable for concrete production. Const Build Mater 65:201–217
2. Etxeberria M, Vázquez E, Marí A et al (2007) Influence of amount of recycled coarse aggregates and production process on properties of recycled aggregate concrete. Cem Concr Res 37(5):735–742
3. Yang YF, Han LH (2006) Experimental behaviour of recycled aggregate concrete filled steel tubular columns. J Constr Steel Res 62(12):1310–1324
4. Wu B, Zhao XY, Zhang JS et al (2012) Seismic tests on square thin-walled steel tubular columns filled with demolished concrete lumps. Key Eng Mater 517:958–967
5. Xiao J, Li W, Fan Y et al (2012) An overview of study on recycled aggregate concrete in China (1996–2011). Constr Build Mater 31:364–383
6. Topcu IB, Şengel S (2004) Properties of concretes produced with waste concrete aggregate. Cem Concr Res 34(8):1307–1312
7. Yang YF, Hou C (2015) Behaviour and design calculations of recycled aggregate concrete-filled steel tube (RACFST) members. Magaz Concr Res 67(11):611–620
8. Konno K, Sato Y, Kakuta Y et al (1998) The property of recycled concrete column encased by steel tube subjected to axial compression. Trans Japan Concr Inst 19:231–238
9. Xiao J, Huang Y, Yang J et al (2012) Mechanical properties of confined recycled aggregate concrete under axial compression. Const Build Mater 26(1):591–603
10. Schneider SP (1998) Axially loaded concrete-filled steel tubes. J Struct Eng 124(10):1125–1138
11. Chen Z, Xu J, Xue J et al (2014) Performance and calculations of recycled aggregate concrete-filled steel tubular (RACFST) short columns under axial compression. Int J Steel Struct 14(1):31–42
12. Liu J, Wang X, Zhang S (2015) Behavior of square tubed reinforced-concrete short columns subjected to eccentric compression. Thin-Walled Struct 91:108–115
13. Yang YF, Han LH, Wu X (2008) Concrete shrinkage and creep in recycled aggregate concrete-filled steel tubes. Adv Struct Eng 11(4):383–396
14. Ajdukiewicz A, Kliszczewicz A (2002) Influence of recycled aggregates on mechanical properties of HS/HPC. Cem Concr Compos 24(2):269–279
15. Portoles JM, Serra E, Romero ML (2013) Influence of ultra-high strength infill in slender concrete-filled steel tubular columns. J Constr Steel Res 86:107–114
16. Ma H, Xue J, Zhang X et al (2013) Seismic performance of steel-reinforced recycled concrete columns under low cyclic loads. Constr Build Mater 48:229–237
17. Silva A, Jiang Y, Macedo L et al (2016) seismic performance of composite moment-resisting frames achieved with sustainable CFST members. Front Struct Civ Eng 10(3):312–332
18. Teng JG, Zhao JL, Yu T et al (2012) Recycling of coarsely-crushed concrete for use in FRP tubular columns. In: Proceedings of the First International Conference on Performance-Based and Life-Cycle Structural Engineering, 2012, pp 1389–1397
19. Liu F, Yan Y, Li LJ (2012) Experimental study on impact performance of recycled plastic reinforced concrete. In: Proceedings of the First International Conference on Performance-Based and Life-Cycle Structural Engineering 2012, pp 1409–1421
20. DG/TJ 08-2018-2007 (2007) Technical specification for application of recycled concrete. Shanghai (**in Chinese**)
21. DB34/T 1262-2010 (2010) Technical specification for concrete-filled steel tubular structures. Hefei (**in Chinese**)
22. JGJ101-96 (1996) Specification of testing methods for earthquake resistant building. China Architecture and Building Press, Beijing (**in Chinese**)
23. CECS 28:90 (1990) Design and construction specification for concrete-filled steel tubular structures. China Planning Press, Beijing (**in Chinese**)
24. Xiao JZ, Li WG, Fan YH et al (2012) An overview of study on recycled aggregate concrete in China (1996–2011). Constr Build Mater 31:364–383